Deformation mechanisms and damage of oxide dispersion strengthened steels at high temperature

A. Steckmeyer, Benjamin Fournier, J. Malaplate, M. Praud, I. Tournié, Samuel Forest

DEFORMATION MECHANISMS AND DAMAGE OF OXIDE DISPERSION STRENGTHENED STEELS AT HIGH TEMPERATURE

A. Steckmeyer[1)], B. Fournier[1)], J. Malaplate[1)], M. Praud[1)], I. Tournié[1)], S. Forest[2)]
[1)] CEA, DEN/DANS/DMN/SRMA, commissariat à l'énergie atomique, 91191 Gif-sur-Yvette, France
[2)] Centre des matériaux, Mines ParisTech, 91003 Evry, France

ABSTRACT

A ferritic oxide dispersion strengthened steel is under study for fuel cladding applications in future nuclear systems. Tensile tests and creep tests are carried out at various temperatures to determine its mechanical properties along the extrusion direction. For these two types of loading, the material exhibits a high mechanical resistance. Its ductility appears to be strongly influenced by the strain rate and the temperature. Deformation mechanisms linked to diffusion phenomena are suspected and intergranular damage is observed on fractured specimens.

KEYWORDS

ODS steels, high temperature, tension, creep, damage, strain rate effect.

INTRODUCTION

Ferritic and martensitic oxide dispersion strengthened (ODS) steels are known for both their excellent high temperature creep resistance and their low irradiation swelling [1-2]. Therefore, they are of first interest for nuclear fission reactors. More precisely, they appear as the most promising candidates - as cladding materials - to meet the specifications for the generation IV of nuclear systems. These specifications demand an increase of the operating temperature and of the fuel combustion rate. By the end of their in-service operation time, the cladding tubes will have to face a 100 MPa hoop stress and a 200 dpa dose.

In this study, the tensile and creep properties of J05 alloy, an ODS ferritic steel produced by hot extrusion at CEA are presented. Its mechanical properties are evaluated from room temperature to 750℃ in tension, and at 650℃ in cr eep. The effect of strain rate is especially studied. Post-mortem observations using scanning electron microscopy (SEM) are conducted to study deformation mechanisms and damage.

SPECIMEN, MATERIAL AND TESTING

Material

The nominal composition of the ODS steel under study is Fe-14Cr-1W-0.26Ti-0.3Y_2O_3 (in wt %). Firstly, a pre-alloyed powder and an yttria powder were mechanically alloyed. The resulting powder was then canned, degassed at 300℃ and hot extruded at 1100℃. Finally, the 16 mm diameter rod produced was annealed at 1050℃ for 1 hour. Its mean hardness value under a 0.1 kg load is 434 HV.

Due to the consolidation process, grains are elongated along the extrusion direction. Their mean length is 1.2 µm and their mean width is about 550 nm (Fig. 1). Texture analyses conducted with both electron-back scattering and X-ray diffraction revealed that this morphological texture was coupled with a pronounced orientation texture [3]. For a large majority of grains, the extrusion direction is oriented along a <110> crystallographic direction. Transmission electron microscopy (TEM) showed that the distribution of nano-particles was homogeneous. Their mean size is 2.3 nm and their density amounts to 5.10^{22} m^{-3}. Some larger particles (from 100 nm to 1 µm) were also observed on some grain boundaries. They appear to be aligned along the extrusion direction and are titanium-rich and/or aluminium rich, as described in [4] on another 14Cr ODS steel.

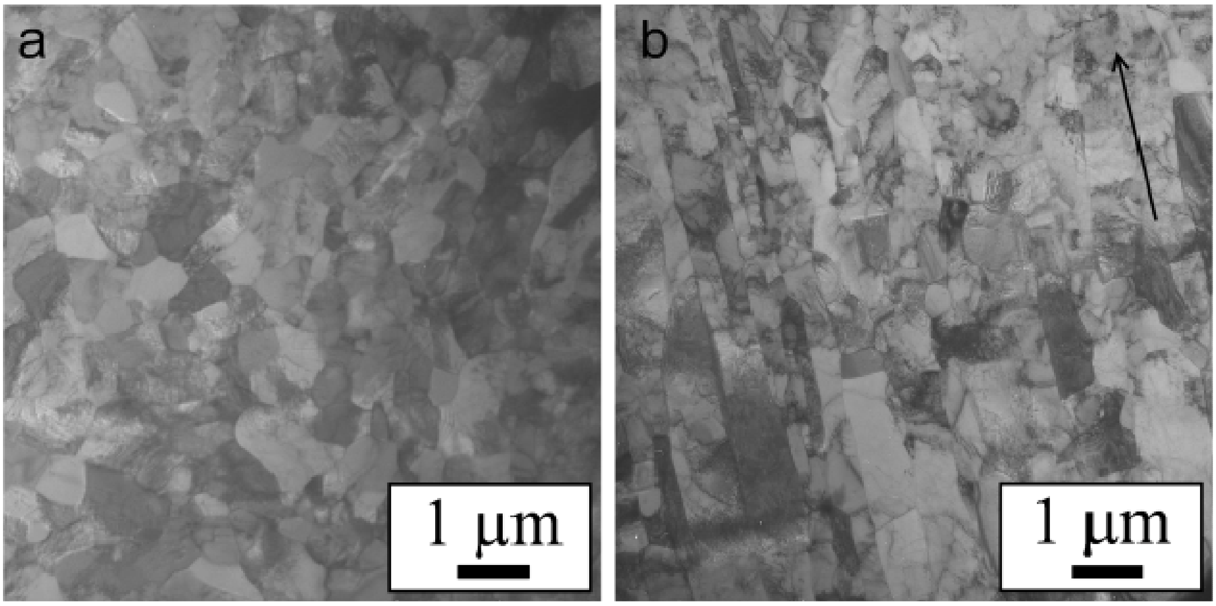

Fig. 1: TEM images of the as-received microstructure of J05 ODS steel. Extrusion direction is perpendicular to the observed plane in (a) and along the arrow in (b).

Testing

The same specimen geometry was used for tensile tests and creep tests. It had a gauge length of 6 mm, a circular section of 3 mm diameter and an axial direction parallel to the extrusion direction. Tensile tests were carried out in air at temperatures ranging from 25°C to 750°C. They were strain controlled with strain rates between 10^{-2} s^{-1} and 10^{-5} s^{-1}. Tensile results presented here also include results from [5]. Creep tests were conducted in air at 650°C and at different (constant) loads.

EXPERIMENTAL RESULTS

Tensile tests

The evolution with respect to temperature of the ultimate tensile strength (R_m) of J05 ODS steel is described in Fig. 2a. It decreases from 1180 MPa at room temperature to 340 MPa at 750°C, this decrease being steeper above 400°C. A strain rate effect is noticed: the higher the strain rate, the higher the tensile strength. This moderate effect is maximum at 550°C.The evolution of the yield strength (R_p) is described on the same figure and is very similar. It shows that the strain hardening of the alloy under study is very limited: it reaches a maximum value of 10% at room temperature (and high strain rate) and decreases at higher temperature.

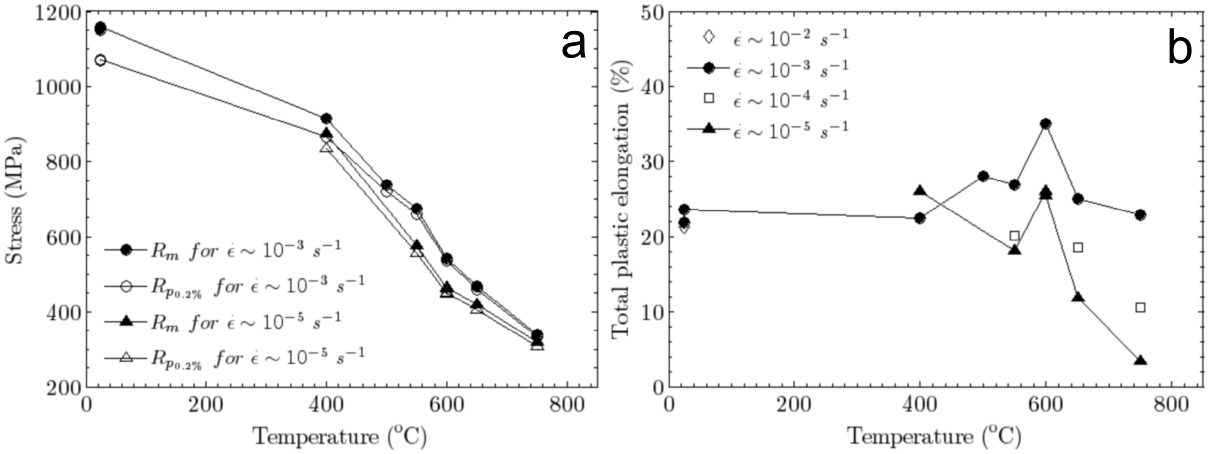

Fig. 2: Evolution of (a) the ultimate tensile strength (R_m) and yield strength ($R_{p\ 0.2\%}$) and (b) of the total plastic elongation according to the temperature and for various strain rates. J05 steel.

The evolution of the plastic elongation at fracture is given in Fig. 2b. At relatively high strain rate ($10^{-3}\ s^{-1}$) the ductility of J05 steel remains higher than 20% on the whole range of tested temperatures. A peak of ductility is observed at 600℃. Above 400℃, a strong influence of the strain rate is noticed. Indeed, the lower the strain rate, the lower the ductility. Therefore, even if a total plastic elongation of 22.9% is reached at 750℃ for a strain rate of $10^{-3}\ s^{-1}$, this value falls down to 3.4% at the same temperature but at a lower strain rate ($10^{-5}\ s^{-1}$). Above 600℃, the strain rate and temperatures effects com bine: both a decrease of the strain rate and an increase of the temperature lead to a reduced total plastic strain.

The value of the plastic strain at the very moment at which the necking occurs was measured for every tensile test. The evolution of this homogeneous plastic strain - according to the strain rate and temperature - exhibits the exact same trends as mentioned above for the total plastic strain. Therefore, it can be stated that the temperature and strain rate effects described earlier affect the homogeneous behaviour of the ODS steel under study.

Creep tests

Four creep tests were carried out for the present study, at respectively 220, 300, 330 and 350 MPa. The four specimens were tested at 650℃. U p to now, and after more than 5000 hours of creep, no fracture occurred.

DISCUSSION

Tensile properties

Fig. 3 gathers the tensile properties of various ODS ferritic steels available in literature. These data correspond to tensile tests carried out at relatively high strain rates (around $10^{-3}\ s^{-1}$). Values corresponding to J05 steel are also included. Fig. 3a shows that the alloy under study is the most ductile ODS steel on almost the whole range of tested temperatures. Fig. 3b reveals that it lies among the most resistant nano-strengthened steels. Therefore, J05 steel exhibits an excellent compromise between strength and ductility.

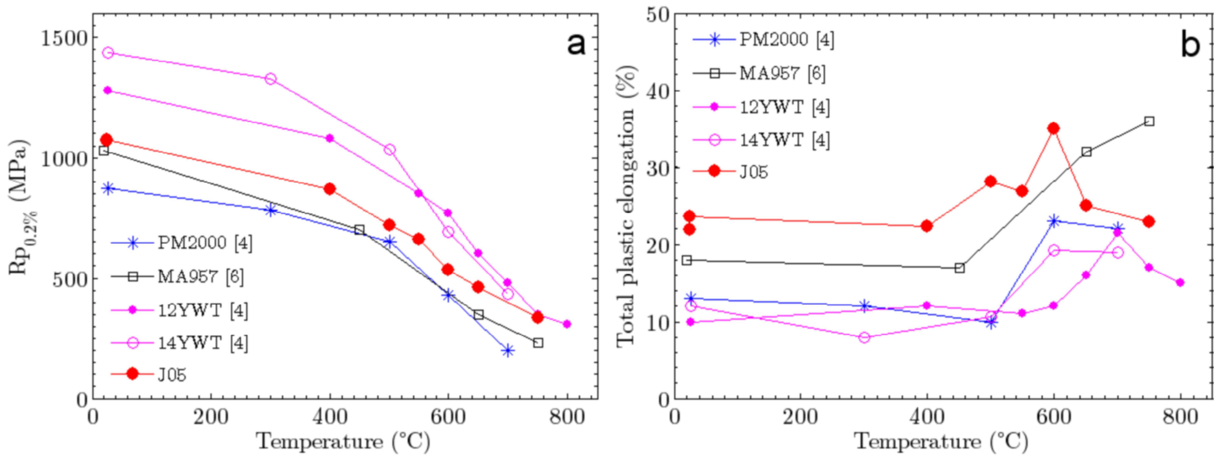

Fig. 3: Evolution of (a) the ultimate tensile strength (R_m) and yield strength ($R_{p\ 0.2\%}$) and (b) of the total plastic elongation according to the temperature and for various strain rates. Various ferritic ODS steels of literature.

A common property of ODS steels is found in Fig. 3b: a peak of ductility exists for nearly every grade of ODS steel reported here. MA957 is the only grade for which a lack of data at high temperature prevents from concluding. This peak of ductility (with respect to the temperature) occurs at 600°C or above, depending on the grade. It may be accounted for by a competition between distinct deformation mechanisms. Such a competition could oppose mechanisms governing viscoplasticity, which would tend to enhance the total strain, to vacancy diffusion along grain boundaries, synonym of damage and thus reduced total strain. As a small grain size promotes vacancy diffusion, one may expect that the smaller the grain size, the lower the temperature of the peak of ductility (and similarly with a high dislocation density). Unfortunately, a much more precise determination of the temperature of the peaks is needed to confirm the correlation between grain size, dislocation density and temperature of maximum total strain.

Creep properties

Even if creep tests are still in progress, it is already possible to draw some conclusions on the behaviour of J05 ODS steel under creep along the extrusion direction. Fig. 4a compares the lifetime under creep at 650°C of several ODS steels. The MA957 ODS alloy, a commercial ODS produced by *Inco*, is used as the reference. It turns out that J05 steel is much more resistant to creep than MA957 since at high stress levels, some specimens already exhibit lifetimes longer by more than one order of magnitude. A Larson-Miller diagram (Fig. 4b) enables a wider comparison with available experimental data. The conclusion on J05 creep strength is the same since specimens under creep at high stress levels (330 and 350 MPa) are almost already more resistant than other experimental ODS alloys. Minimum creep rates at 650°C are given in Fig. 4c for the same ferritic ODS. Once again, it appears that the minimum creep rates of high stressed J05 specimens are (already) lower than the corresponding minimum creep rates of MA957.

In Fig. 4c, results from creep tests carried out on MA957 at 700°C are also reported. They show that the stress exponent in Norton's creep law (on minimum creep rate) is identical between 650°C and 700°C. In fact, this exponent has the same value on the whole range 600°C – 700°C, as reported in [7]. This observation tends to prove that deformation mechanisms are identical for creep tests of ODS steels between 600°C and 700°C. This point is of first interest in order to shorten creep tests by increasing the tests temperature, without modifying the underlying creep deformation mechanisms.

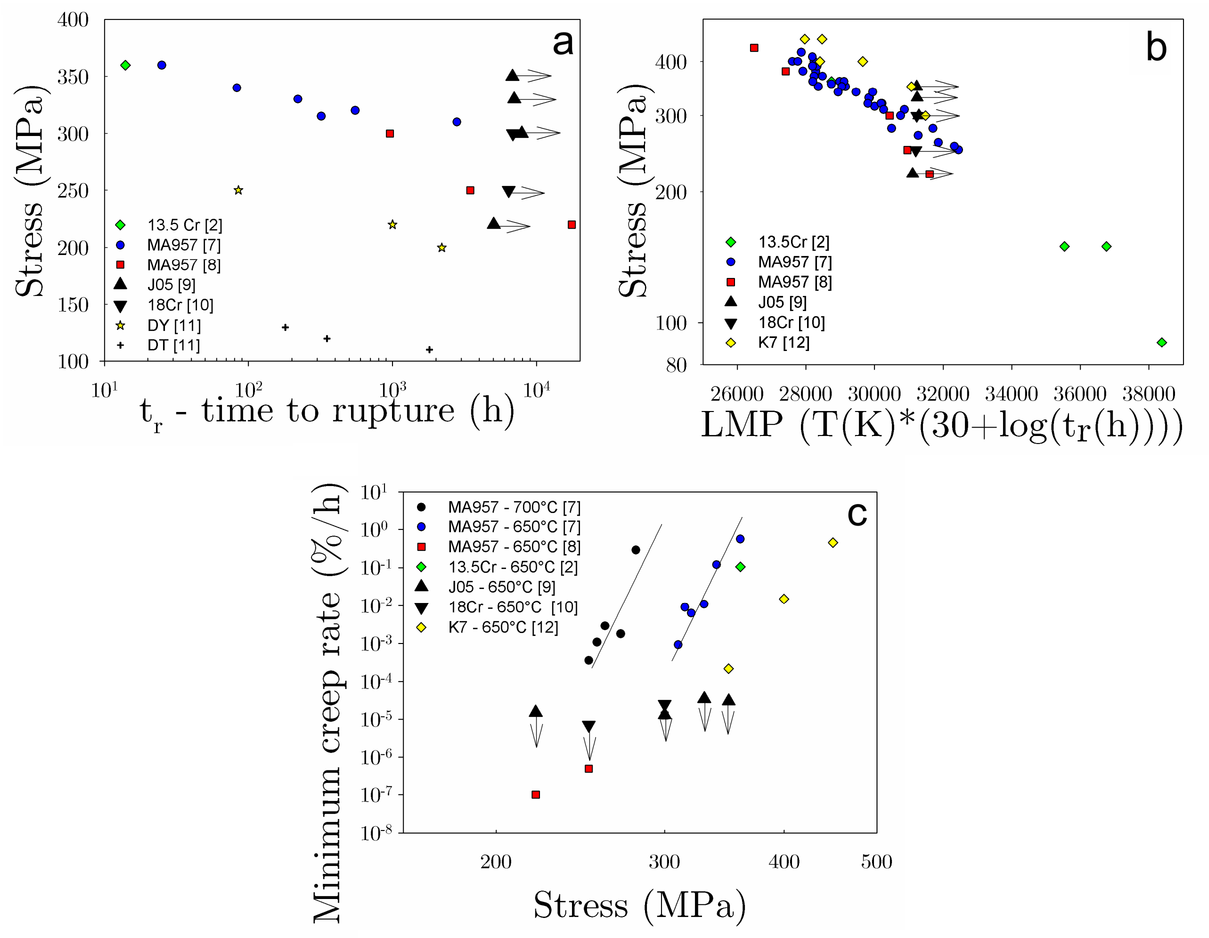

Fig. 4: Creep results for different ferritic ODS steels. Lifetime diagram at 650℃ (a), Larson-Miller diagram for temperatures between 600℃ and 900℃ (b) and minimum creep rate diagram at 650℃ (and 700℃) (c).

Deformation mechanisms and damage

Tensile results reported above on J05 ODS steel state that beyond 600℃, both a rise of the temperature and a decrease of the strain rate lead to a reduced total (and homogeneous) elongation. This is in complete agreement with the low values of total elongation observed after creep rupture and reported in literature [13]. A change in the deformation mechanisms is thus suspected at high temperature and low strain rates, conditions which are usually associated with diffusion.

The suspicion of an evolution of deformation mechanisms is justified by the observation of two types of damage on the fracture surface of tensile specimens. Fig. 5a represents a typical fracture surface. Two different areas can be distinguished: a rugged central area and a smoother outer area, with a different inclination relative to the loading direcction. In the latter, well defined dimples can be observed (Fig. 5b and Fig. 5c), while in the former, an intergranular decohesion is noticed, as seen in Fig. 5d and particularly in Fig. 5e. No particle was observed inside the dimples of Fig. 5b, which present a slight oxidation. In Fig. 5e, ligaments of ductile tearing surround zones where the intergranular decohesion occurred. Analysis of the fracture surfaces shows that, at a given strain rate, the fraction of the surface where intergranular decohesion is observed increases with increasing temperature. Hence, the mechanism of intergranular decohesion appears to be promoted at high temperature.

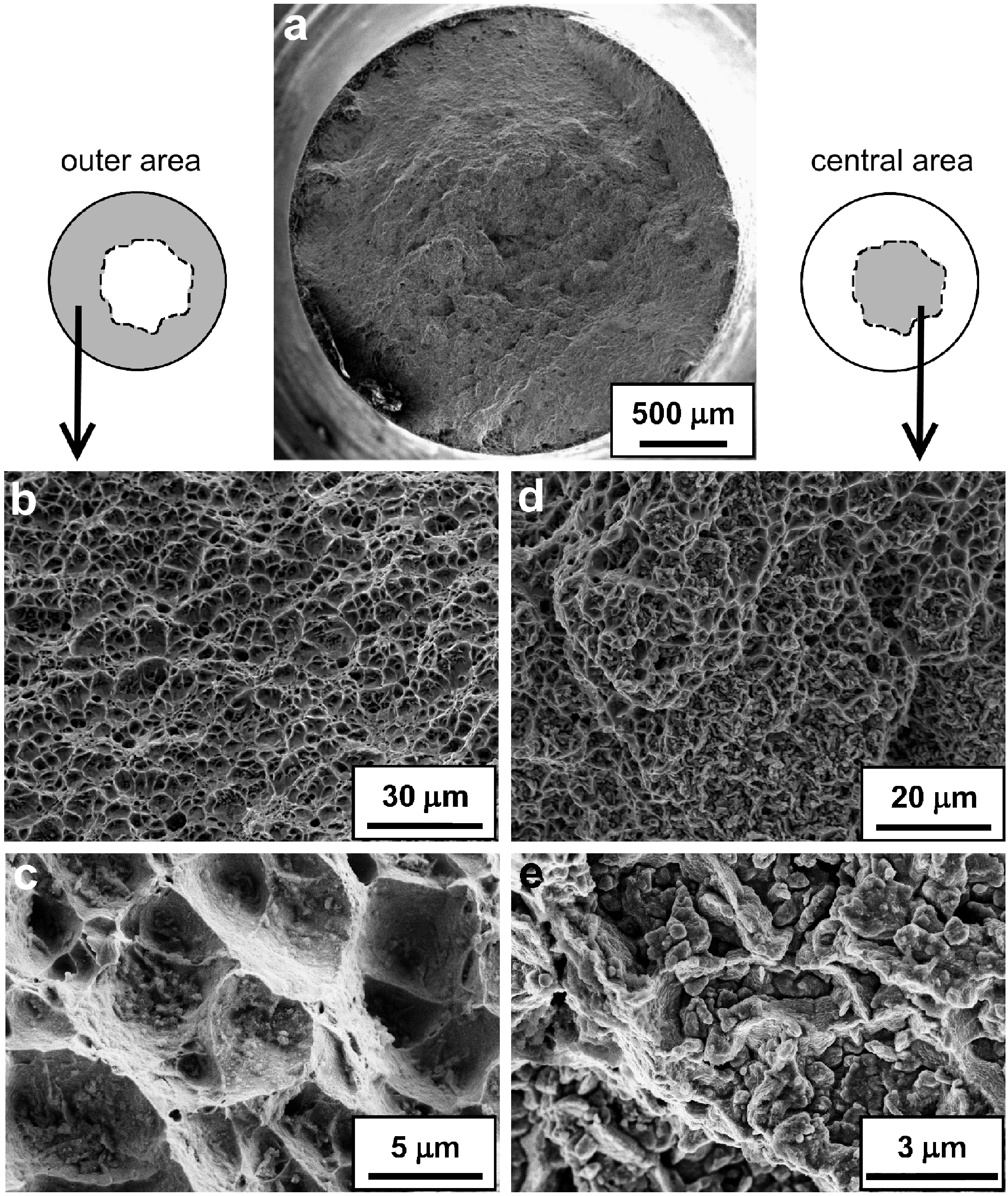

Fig. 5: SEM images of the fracture surface of a J05 specimen tested in tension at 650°C and 10^{-5} s^{-1}. Overall view (a) and zooms in the outer area (b,c) and in the central area (d,e). The two schemes describes respectively the outer are where dimples are predominant (left) and the central area where intergranular decohesion is observed (right).

Damage was also observed on longitudinally cut specimens. Fig. 6 reveals cavities located relatively far from the fracture surface. Some cavities are located at the edge of grains and are elongated perpendicular to the loading/extrusion direction. Some other cavities are observed along grains boundaries, aligned with the stringer-like Ti-rich particles.

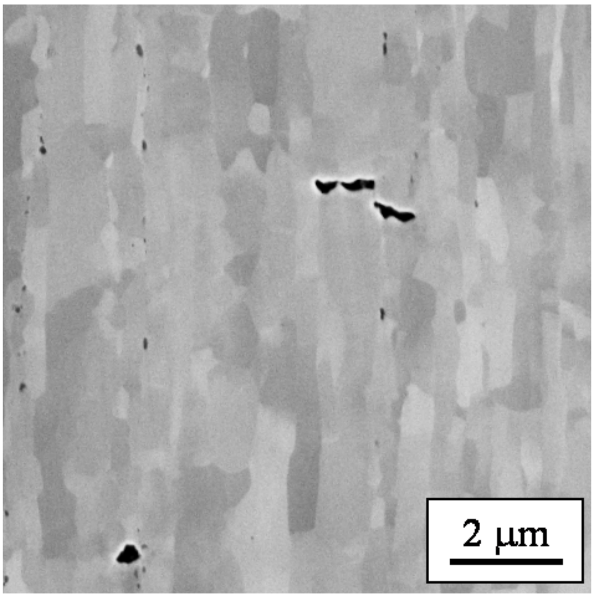

Fig. 6: SEM observation of a longitudinally cut J05 tensile specimen. The extrusion/loading direction is vertical. Cavities are surrounded by a white halo.

Brittleness of grain boundaries may also be critical at lower temperature since many secondary cracks (cracks perpendicular to the section of the specimen) were observed on the fractured surface of specimens tested in tension at room temperature.

CONCLUSIONS

In this study, the mechanical properties of a 14% chromium ferritic oxide dispersion strengthened steel were evaluated in tension and creep along the extrusion direction. The results prove the high tensile strength and high creep resistance of the alloy under study between 25℃ and 750℃. The ductility of the materi al turns out to be remarkable at high strain rate, compared to other ODS steels. It exhibits a peak at 600℃. However, beyond 400℃, ductility decreases sharply with decreasing strain rate. The expected total strain of creep specimens is thus very small, as reported in literature. Deformation mechanisms promoted by diffusion phenomenon may account for this strongly-reduced ductility at high temperature (above 600℃) and low strain rate. Inve stigations of fracture surfaces revealed two types of damage occurred: a typical dimple growth ductile mechanism and an intergranular decohesion. The intergranular decohesion increases with the temperature.

REFERENCES

[1] Huet, J.J.:
Preparation and properties of oxide dispersion-strengthened ferritic alloys
Metal Powder Report, 40 (1985), pp. 155-158

[2] Mukhopadhyay, D.K.; Froes, F.H.; Gelles, D.S.:
Development of oxide dispersion strengthened ferritic steels for fusion
Journal of Nuclear Materials, 258 (1998), pp. 1209-1215

[3] Bougault, A.; Malaplate, J.; Fournier, B. et al.:
Caractérisation microstructurale et mécanique des ODS CEA
CEA internal report

[4] Klueh, R.L.; Shingledecker, J.P.; Swindeman, R.W.; Hoelzer, D.T.:
Oxide dispersion-strengthened steels: a comparison of some commercial and experimental alloys
Journal of Nuclear Materials, 341 (2005), pp. 103-114

[5] Praud, M.:
Analyses microstructurales et comportement en traction d’aciers ODS
Master thesis, Institut National Polytechnique de Toulouse, 2009

[6] Réglé, H.:
Alliages ferritiques 14/20% de chrome renforcés par dispersion d’oxydes
Ph. D. thesis, Université Paris XI, 1994

[7] Wilshire, B.; Lieu, T.D.;
Deformation and damage processes during creep of Incoloy MA957
Material Science and Engineering A, 386 (2004), pp. 81-90

[8] Alamo, A.; Lambard, V.; Averty, X.; Mathon, M.H.:
Assessment of ODS-14%Cr ferritic alloy for high temperature applications
Journal of Nuclear Materials, 329 (2004), pp. 333-337

[9] Steckmeyer, A.:
Caractérisation et modélisation du comportement mécanique à haute temperature des aciers nano-renforcés
Master thesis, Ecole Normale Supérieure de Cachan, 2009

[10] Ratti, M.:
Développement de nouvelles nuances d’aciers ferritiques / martensitiques pour le gainage d’éléments combustible des Réacteurs à Neutrons Rapides au sodium
Ph. D. thesis, Institute National Polytechnique de Grenoble, 2009

[11] Zakine, C.:
Plasticité des alliages ferritiques renforcés par dispersion d’oxydes
Ph. D. thesis, Ecole Centrale de Paris, 1994

[12] Sagaradze, V.V. et al.:
Radiation resistance and thermal creep of ODS ferritic steels
Journal of Nuclear Materials, 295 (2001), pp.265-272

[13] Sagasegawa, H. et al:
Creep constitutive equation of dual phase 9Cr-ODS steel
Journal of Nuclear Materials, 373 (2008), pp. 82-89

Corresponding author: antonin.steckmeyer@cea.fr